Structural Engineering and Mechanics, Vol. 43, No. 5 (2012) 623-636
DOI: http://dx.doi.org/10.12989/sem.2012.43.5.623

Behaviour of fiber reinforced concrete beams with spliced tension steel reinforcement

Mohamed A. Safan*

Civil Engineering Department, Faculty of Engineering, Menoufia University, Shebeen El-Koom, 1111 Menoufia, Egypt

(Received December 26, 2011, Revised July 12, 2012, Accepted August 9, 2012)

Abstract. The aim of the current work is to describe the flexural behaviour of simply supported concrete beams with tension reinforcement spliced at mid-span. The parameters included in the study were the type of the concrete, the splice length and the configuration of the hooked splice. Fifteen beams were cast using an ordinary concrete mix and two fiber reinforced concrete mixes incorporating steel and polypropylene fibers. Each concrete mix was used to cast five beams with continuous, spliced and hooked spliced tension steel bars. A test beam was reinforced on the tension side with two 12 mm bars and the splice length was 20 and 40 times the bar diameter. The hooked bars were spliced along 20 times the bar diameter and provided with 45-degree and 90-degree hooks. The test results in terms of cracking and ultimate loads, cracking patterns, ductility, and failure modes are reported. The results demonstrated the consequences due to short splices and the improvement in the structural behaviour due to the use of hooks and the confinement provided by the steel and polypropylene fibers.

Keywords: bond; splice; hook; fiber reinforced concrete; steel fibers; polypropylene fibers

1. Introduction

The monolithic behaviour of reinforced concrete elements and transfer of stress is based on bond between the reinforcing steel and the surrounding concrete. Cracking and crack width, deflections, strength and energy absorption are all related directly or indirectly to bond strength. Efficient bond ensures reliable force transfer between the reinforcement and the surrounding concrete. In the case of a deformed steel bar, the following mechanisms contribute to force transfer: (1) Chemical adhesion between the bar and the concrete, (2) Frictional forces arising from the roughness of the interface and (3) Mechanical anchorage or bearing of the ribs against the concrete surface (ACI 408R 2003). Bond strength has been recently treated as a structural property rather a material property. It has been demonstrated that the bond strength is governed by the mechanical properties of the concrete, the volume of the concrete around the bars in terms of the concrete cover and bar spacing parameters; the presence of confinement in the form of transverse reinforcement, which can delay and control crack propagation, the diameter and geometry of the bar (bar diameter, deformation height, spacing, width, and face angle) and the loading regime (monotonic or cyclic

*Corresponding author, Associate Professor, E-mail: msafan2000@yahoo.com

and the loading history and rate) (ACI 408R 2003, FIB 2000, Turk 2003, Turk *et al*. 2005).

Bond failure between steel and concrete is generally characterized by two modes, namely pullout and splitting. If the ratio of the concrete cover to the bar diameter is relatively large or the concrete is well confined, bond failure occurs in pullout mode due to the shearing off of the concrete keys between the bar ribs. On the other hand, if the concrete cover is small or the steel bars are closely spaced, tensile splitting cracks tend to develop under the radial component of the rib bearing forces parallel to the steel bars causing premature bond failure (ACI 408-2R-92 2005). For most structural applications, bond failures are governed by splitting of the concrete rather than by pullout. Actually, the provisions in ACI 318R (2008) for the development of deformed bars are based on bond strengths governed by a splitting failure of the concrete around the bar. The average bond strength at splitting bond failure is influenced by several parameters such as the ratio of the concrete cover to bar diameter, the development or splice length, the concrete compressive strength and concrete confinement (Zuo 2000, ACI 408.3/408.3R 2001).

One of the most practical and effective means for improving the bond strength of steel bars is concrete confinement. Concrete confinement becomes particularly important with the more frequent use of high strength concrete and also in the areas of seismic hazards for improving the ductility of bond failure and enhancing the energy absorption and dissipation capabilities of the structure (Azizinamini 1993, Esfahani 1998, Harajli 2004, 2006, Mehmet 2010). The most common method for concrete confinement is the use of closely spaced ties or hoops within the development or splice region. Transverse reinforcement confines the developed and spliced bars by limiting the progression of splitting cracks and, thus, increasing the bond force required to cause failure. The increase in transverse reinforcement results in an increase in bond force and eventually converting a splitting failure to a pullout failure (Darwin 1993).

Another method that has been gaining interest involves the use of steel ber reinforced concrete. Different types of reinforcing fibers can be incorporated to improve the resistance to splitting cracks and reduce the required development lengths (ACI 544.1R-96 2002). Steel and polypropylene fibers were the most commonly used types in previous research work. The bond tests for normal and high strength concrete mixes were performed on pullout specimens as well as splice specimens. According to pullout test results (Ezeldin 1989, Harajli 1995, Soroushian 1994), it was found that longer steel fibers (up to 90 mm) resulted in higher bond strengths. The increase in the fiber content and length resulted in improved post-peak ductility. The steel fiber content was typically not less than 0.5% by volume of the concrete mix to cause significant increase in bond strength. The amount of strength gain was higher for bigger bar diameters and the strength gain due to polypropylene fibers was limited to about one third compared to steel fibers in counterpart specimens. According to splice beam test results, it was possible to increase the bond strength by three times when 2% by volume steel fibers were added in high strength concrete beams (Bilal 2001). Also, it was found that the presence of fibers increased the number of cracks formed around the splices, delayed splitting cracks, and improved the ductility of members undergoing a bond failure (Leung 2003). Polypropylene fibers improved the performance in the post splitting range, but had less effect on bond strength (Harajli 1997). These results were attributed to the improved modulus of rupture of the concrete containing steel fibers and the higher strain capacity associated with concrete crushing. On the other hand, the polypropylene fibers would be beneficial in arresting the cracking width in the post splitting stage rather control the initiation of cracks with regard to the low modulus of the polypropylene fibers. Similar enhancement in terms of strength and ductility was achieved in test specimens simulating beam-column connections reinforced with hooked bars due to the addition of steel fibers (Bilal 2011).

Furthermore, concrete confinement for improving ductility and bond strength can be achieved using external fiber reinforced polymer (FRP) systems, which have evolved over the last few decades as a viable alternative to traditional materials and construction techniques (ACI 407R 2007, Thai and Pimanmas 2011). FRP confinement utilized the wrapping technique to adhere U-shaped strips along the spliced length. The tests results demonstrated the efficiency of both glass and carbon fiber laminates of limited thickness to cause significant improvement in the bond strength and ductility (Bilal *et al*. 2004, Harajli 2005, Pimanmas and Thai 2011).

2. Aim and significance of the current work

The primary objective of the experimental research work reported in this paper was to evaluate the effect of fiber reinforcement and the configuration of hooked spliced bras on the flexural behaviour of simply supported beams. An ordinary concrete mix and two fiber reinforced mixes incorporating steel and polypropylene fibers were used to cast three groups of test specimens. Each group consisted of five beams; one beam was reinforced with continuous tension bars, while the bars in the other four beams were lap spliced at midspan. The splice length in two beams was 20 and 40 times the bar diameter. The tension bars in the remaining two beams were hooked with a splice length of 20 times the bar diameter. The hooks were formed at 45-degree and 90-dgrees. Thus, the parameters considered were the splice length, type of concrete, type of fibers and the configuration of the hook. The prescribed test scheme made it possible to assess the influence of the individual and combined parameters of the study on the flexural behaviour. The current research significance arises from the fact that the use of fibers affects the failure load of spliced beam specimens by altering the contribution of the concrete to the flexure strength of a section as well as to bond. Based on the current literature, it was significant that more work and data are still needed to properly judge the effect of fibers on the structural behaviour of spliced beams.

3. Experimental study

Fifteen test specimens were designed to study the influence of the following parameters on the flexure and bond performance (i) splice length, (ii) concrete type, (iii) type of fibers and (iv) hook configuration. All beams had the same dimensions and the reinforcement ratio. Three concrete mixes (C, P and S) were used in casting the test specimens. Mix (C) is an ordinary control mix without fibers, mix (P) is a polypropylene fiber reinforced mix and mix (S) is a steel fiber reinforced concrete mix. Two 12 mm tension steel bars were used as main reinforcement. Test beams were designated by the concrete mix, splice length indication and the hook configuration. A beam designated as S20/45 was cast using mix (S) and the splice length was 20 times the bar diameter with a 45- degree hook.

3.1 Design considerations

The reinforcement ratio in all test beams was 1.26%. The shear reinforcement provided a shear strength that was theoretically about two times the flexure strength of the control beam (C) to ensure safety against shear failure. The reinforcement ratio was 55 percent of the balanced ratio according to the ACI 318R-08 code, Eq. (B-1) (ACI 318R 2008). The development length l_d is calculated according to the following ACI 318R-08 equation (Eq. (12-1)

$$l_d = [(3/40)\ (f_y\ /\lambda\ (f_{cy}{}^{0.5})\ (\psi_t\ \psi_e\ \psi_s)/((c_b + K_{tr})/d_b)]d_b \tag{1}$$

In which:

l_d : development length, in. (1 in = 25.4 mm).
f_y : yield strength, psi (f_y not more than 60, 000 psi, 1 psi = 6.895 × 10^{-3} MPa).
f_{cy} : concrete compressive strength, psi.
λ : lightweight concrete factor (1.0 for normalweight concrete).
ψ_t : reinforcement location factor (1.0 for concrete less than 12 in. below the splice).
ψ_e : surface coating factor (1.0 for uncoated reinforcement).
ψ_s : bar size factor (0.8 for No. 6 (19 mm) and smaller bars).
c_b : the smaller of the distance from center of bar being spliced to the nearest concrete surface, and one-half the center-to-center spacing of bars being spliced, in.
K_{tr} : transverse reinforcement index (40 A_{tr}/sn, A_{tr}: area of all transverse reinforcement which is within the spacing (s) and crosses the potential plane of splitting through the reinforcement being spliced (in^2), s: stirrup spacing (in) and n: No. of spliced bars (K_{tr} not more than 2.5).
d_b : nominal diameter of the bar, in.

Applying the above values of the ψ_t, ψ_e, ψ_s factors yields

$$l_d = [(3/50)\ (f_y\ /\lambda\ (f_{cy}{}^{0.5})\ ((c_b + K_{tr})/d_b)]\ d_b \tag{2}$$

The term $(c_b + K_{tr})/d_b$ accounts for the effects of small cover, close bar spacing, and confinement provided by transverse reinforcement. When $(c_b + K_{tr})/d_b$ is less than 2.5, splitting failures are likely to occur. For values above 2.5, a pullout failure is expected and an increase in the cover or the transverse reinforcement is unlikely to increase the anchorage capacity (ACI 318R 2008). Therefore, a limit value of 2.5 was specified to safeguard against pullout type failures. According to the material properties and the dimensions given in Table 1 the limit value of 2.5 for $(c_b + K_{tr})/d_b$ was

Table 1 Splice length design cacultions

Parameter	Value
- d_b, spliced bar diameter	12 mm (0.472 in.)
- n (No. of spliced bars)	2
- stirrup diameter	8 mm (0.31 in.)
- s (spacing of stirrups)	100 (3.94 in.)
- cover to the stirrups	6 mm (0.236 in.)
- clear cover	6 + 8 = 14 mm (0.55 in.)
- clear spacing between spliced bars	100-2(14)-4(12) = 24 mm (0.94 in.)
- c_b [min. of : clear cover + d_b/2 and (clear spacing + 2d_b)/2]	14 + d_b/2 = 20 mm (0.787 in)
- A_{tr} (two-branch 8 mm stirrup)	100.57 mm^2 (0.156 in^2)
- K_{tr} (= 40 A_{tr} / ns)	0.79
- $(c_b + K_{tr})/d_b$	3.34

considered and the development length was $22.6d_b$ according to Eq. (2). The splice length should not be less than $1.3l_d$ or $29.4d_b$ as all the tension bars are spliced in the maximum moment region (class B splice) according to the ACI 318R-08 code, section (12.15).

The ACI 318R code (2008) permitted the use of $K_{tr} = 0$ as a design simplification even if transverse reinforcement is present. Also, it is permitted to apply $(c_b + K_{tr})/d_b = 1.5$ provided that the clear spacing of the spliced bars is not less than $2d_b$ and the clear cover is not less than d_b. Actually, these requirements were satisfied in the test beams according to the calculations in Table 1. In case $K_{tr} = 0$, the development length was $33.9d_b$ and the corresponding splice length was $44.1d_b$. In case $(c_b + K_{tr})/d_b = 1.5$, the development length was $37.7d_b$ and the corresponding splice length was $49d_b$. Thus, the ACI318R code (2008) design equations provided two applicable limit values of $29.4d_b$ and $49d_b$ for the splice length to prevent pullout failure. The adopted splice lengths in the current work were $20d_b$ and $40d_b$. The smaller splice length of $20d_b$ was intended to cause premature bond failure in the control beam (C20) and allow further improvement due to the use of fibers and hooks. On the other hand, the longer splice of $40d_b$ was intended to achieve satisfactory load transmission between the spliced bars and to allow the study of further improvement due to the use of fibers and/ or hooks.

Applying a 90-degree hook according to the ACI 318R-08 code can significantly reduce the splice length. The hooked splice length is directly proportional to the yield stress of steel and indirectly proportional to the square root of the compressive strength f_{cy}. The hooked splice length obtained from the ACI 318R code (2008), section (12.5) was $24.5d_b$. This value is reported for the purpose of comparison as the applied 90-degree hook, Fig. 1, is not a standard one. Actually, providing the splice with a standard 90-degree hook would require a test beam with a bigger depth.

3.2 Materials

Portland cement (CEMI: 52.5 N) conforming to the requirements of BS EN 197-1:2000 (BS-EN

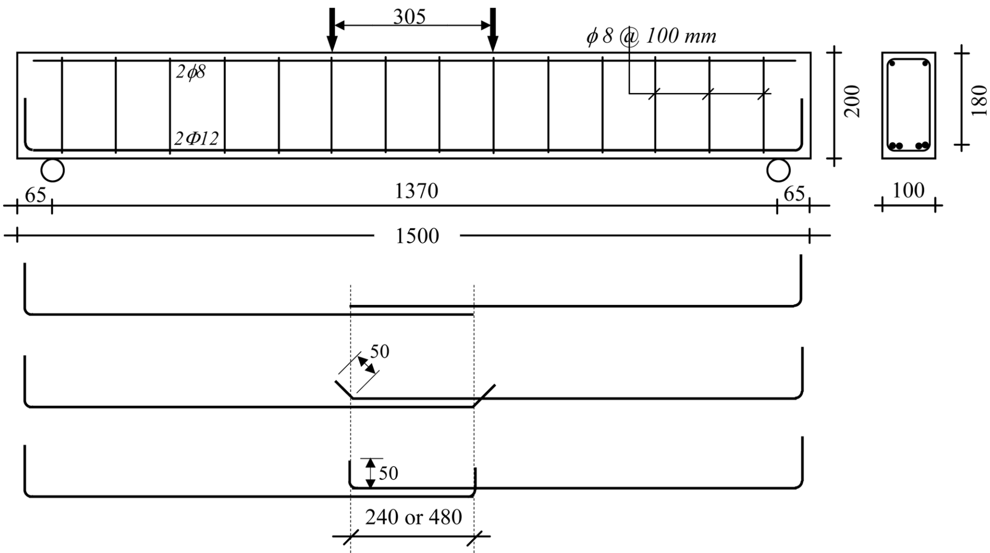

Fig. 1 Geometry of test beams and test configuration

Table 2 Technical data of steel and polypropylene fibers

	Steel fibers	Polypropylene fibers
Tensile strength, MPa	1050	520
Elastic modulus, GPa	210	3.5
Specific weight	7.85	0.9

Fig. 2 Steel and polypropylene fibers

197-1 2000) with a specific gravity of 3.14 and a Blain fineness of 4670 cm^2/g was used. Natural sand having a fineness modulus of 2.6 and a specific gravity of 2.65 was used. Crushed dolomite (specific gravity of 2.65 and crushing modulus of 17.6 percent) with a maximum nominal size of 25 mm was used as coarse aggregates. Deformed steel bras with a nominal diameter of 12 mm and yield strength of 530 MPa were used as tension reinforcement. Stirrups and top reinforcements were made of 8 mm mild steel bars with yield strength of 305 MPa. Steel fibers (NOVOCON®1050) produced by Propex Concrete Systems Corp. – USA were used. The fibers were deformed with hooked ends, 10 mm diameter and 50 mm long. According to the manufacturer, the fibers comply with the requirements of ASTM A820 - type I for cold-drawn wires (ASTM A820). The technical data according to the manufacturer are given in Table 2. Fibrillated 20 mm long polypropylene fibers having a rectangular cross section with an average width of 1.6 mm and average thickness of 0.10 mm were used. This type of fiber, manufactured by Tashi India Limited Company – India, is mechanically distressed or fibrillated to produce main and cross fibril networks forming a lattice pattern. The technical data according to the manufacturer are given in Table 2. Fig. 2 shows the geometry of the used fibers.

3.3 Concrete mix proportions

A 60-liter mixer was used in concrete mixing. The concrete mixes were designed to have a slump of 50 ± 10 mm. The cement content was 350 kg/m^3 in all mixes. The water/cement ratio in the control mix C was 47% provided that the aggregates were used in a saturated surface dry condition. The steel fibers content was 40 kg/m^3 (0.5% by volume). The fibers were added after all other

Table 3 Concrete mix constituents and mechanical properties

Mix	Concrete Constituents, kg/m^3					f_{cy} (MPa)	E_{cy} (GPa)	f_r (MPa)
	Cement	Sand	Dolomite	Water	Fibers			
C	350	690	1245	165	-	32.0	27.6	3.4
P		689	1243	165	4.5	33.5	26.5	3.8
S		675	1220	175	40	35.0	27.9	4.1

constituents had been thoroughly mixed. The fibers were added while the mixer was rotating and mixing continued for about one minute after adding the steel fibers. It was noticed that the slump tended to decrease due to the addition of the steel fibers and the water/cement ratio was increased to 50% to maintain the slump. On the other hand, the addition of the polypropylene fibers did not significantly alter the concrete slump. This was attributed to the smooth texture of the fibers and its relatively small length. The polypropylene fiber content was 4.5 kg/m^3 (0.5% by volume). The fibers were spread and hand mixed after completing the mechanical mixing. The constituents of the three mixes are given in Table 3.

3.4 Preparation and testing of test specimens

Two 30-liter batches were used to cast one beam (100 × 200 × 1500) mm, three cylinders (100 × 200) mm and three prisms (100 × 100 × 500) mm. The cylinders and prisms were tested before testing the beams to determine the compressive stress-strain response and the modulus of rupture, f_r, for each mix. The tests were performed using a 500-kN universal testing machine that enabled an automatic control on the loading range to provide precise load measurements, Fig. 3. The concrete cylinders were loaded by constant displacement increments of 0.04 mm at a loading rate of 0.4 mm/min at which the strain (displacement/specimen height) was plotted against the applied stress (applied load/area of test specimen). The stress-strain relationships are shown in

Fig. 3 Compression test of concrete cylinders

Fig. 4. Each point on a stress-strain curve was the average of three test results. The test results in terms of concrete compressive strength, f_{cy}, modulus of elasticity E_c and the fracture modulus, f_r are given in Table 3.

Tight wooden forms were used to cast the test beams. The inside faces of the forms were greased to prevent water absorption. The specimens were stripped after 24 hours and cured under wet cloth for 7 days and then allowed to dry in the laboratory atmosphere. After 28 days of casting, the test beams were painted in white to facilitate detection of the cracks. The beams were tested under 4-

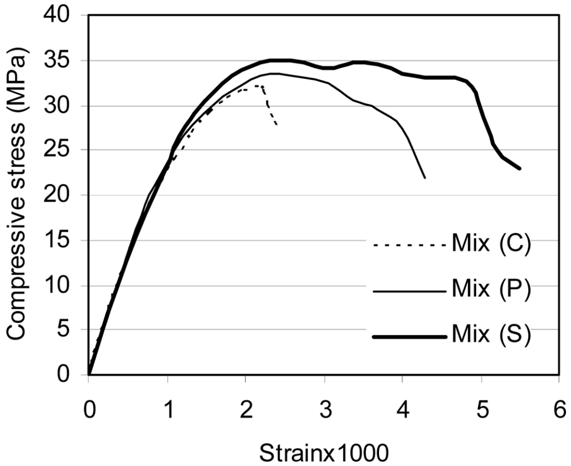

Fig. 4 Compressive stress-strain curves for concrete mixes

Table 4 Experimental test results

Beam	Deflection, mm		Load, kN			Relative P_u	d_u / d_y	No. of cracks	ε_{su}	Failure mode*
	d_y	d_u	P_c	P_y	P_u					
C	14.2	19.5	10	70	71	1.00	1.37	14	0.0036	YC
C40	--	14.0	10	--	66	0.93	--	9	0.0020	B
C20	--	9.10	10	--	52	0.73	--	8	0.0017	B
C20/45	--	12.9	10	--	61	0.84	--	8	0.0018	B
C20/90	10.1	16.3	20	70	75	1.06	1.44	15	0.0029	YC
P	11.9	20.0	15	70	76	1.07	1.68	13	0.0034	YC
P40	--	16.6	15	--	67	0.94	--	15	0.0024	BC
P20	--	16.2	15	--	61	0.86	--	8	0.0022	B
P20/45	14.4	15.5	20	70	71	1.00	1.3	14	0.0030	YC
P20/90	10.0	21.0	20	70	78	1.10	2.1	14	0.0028	YC
S	11.5	21.2	15	75	82	1.16	1.87	12	0.0038	YC
S40	13.8	17.6	15	70	72	1.01	1.27	13	0.0032	YC
S20	--	20.7	15	--	63	0.89	--	12	0.0023	BC
S20/45	10.0	17.1	20	70	76	1.07	1.7	12	0.0029	YC
S20/90	8.98	19.8	20	75	81	1.14	2.2	15	0.0032	YC

*Y: Yield of tension steel, C: Crushing of concrete and B: Bond failure point bending until failure as shown in Fig. 1. The acting load was distributed by means of a rigid beam. The distance between the distributed loads was 305 mm allowing a shear span of 532 mm. The load was applied at constant increments of 5.0 kN utilizing a 100 kN capacity hydraulic flexure machine. The mid-span deflection was measured using a dial gage and the cracks were detected after each load increment. The tensile strain in the reinforcement was measured by means of a 200 mm gage length demountable extensometer. Punched cupper disks were affixed 200 mm center-to center to both sides of each test specimen at the level of the reinforcement. Three disks were affixed in the case of the unspliced beams and those with a short splice to measure the strain along 400 mm, while four disks were affixed in the case of a long splice to measure the strain along 600 mm. Strain measurements were needed to identify yielding of the reinforcement in order to describe the mode of failure. A tensile strain of 0.0026 defined the onset of yielding provided that the yield strength of steel was 530 MPa and assuming a modulus of elasticity of 205 GPa. The tensile strains in the reinforcement at failure (ε_{su}) are reported in Table 4.

4. Test results and discussion

Fifteen test specimens were designed with adequate shear strength to study the influence of lap splicing the tension reinforcement on the structural behaviour of simply supported beams and to describe remedies for improving the structural behaviour by using fibrous concrete and/or deformed hooked bars.

4.1 Stress-strain relationships

Fig. 4 shows the compressive stress-strain curves for test cylinders cast using mixes C, P, and S. The control mix C without fibers demonstrated a traditional brittle failure and a strain of 2.21×10^{-3} at ultimate load. Adding the 20 mm long polypropylene fibers in mix P at a content of 0.5% by volume enabled a considerably less steep descending portion of the stress-strain curve and a marginal increase in the strain at the peak stress compared to mix C. Adding the 50 mm hooked steel fibers in mix S at a content of 0.5% by volume provided a substantial increase in the strain at the peak stress. The measured strain at peak stress was 3.7×10^{-3} associated with a steeper descending branch compared to mix P. The measured compressive strength was 5 and 9 percent higher in mixes P and S, respectively, compared to the control mix. The initial tangent modulus was almost the same for the three mixes.

4.2 Cracking pattern and mode of failure

Fig. 5 shows the cracking patterns of test specimens upon failure. Unspliced beams C, P and S began to crack within the maximum moment region. As the load increased, the cracks propagated towards the compression zone and new cracks developed outside the maximum moment region. Beams C, P and S failed due to yielding of the tension reinforcement followed by concrete crushing within the maximum moment region. The cracking patterns of beams C40 and C20 were remarkably different from that in beam C. The first cracks appeared outside the splice region. As the load increased, the cracks propagated upwards and inclined towards the nearest acting load. Later, shorter cracks developed along the splice length. Strain measurements indicated that the

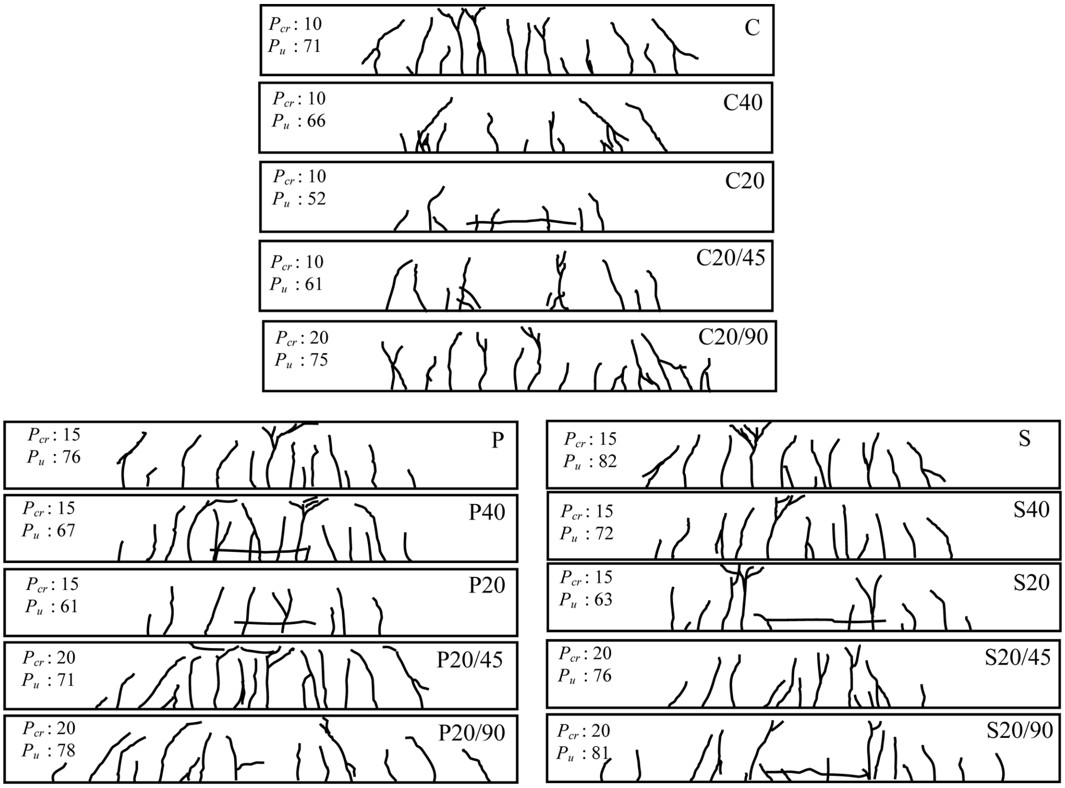

Fig. 5 Cracking patterns of test beams upon failure

tension reinforcement in beams C40 and C20 did not yield before failure that was sudden due to lack of bond. The failure was associated with the appearance of a splitting crack along the splice in beam C20 and the formation of secondary local cracks at the two ends of the splice in beam C40. Providing a 45-degree hooked splice in beams C20/45 did not significantly alter the cracking pattern and mode of failure. However, local inclined cracks aligned with the bent end of the spliced bars rather a longitudinal splitting crack developed at failure. The total number of flexure cracks at failure is reported in Table 4. It can be seen that a considerably smaller number of cracks developed in beam C40, C20 and C20/45 compared to beams C. Providing a 90-degree hooked splice in beam C20/90 seemed to be effective in altering the mode of failure from a premature bond failure to a ductile failure due to yielding of tension steel followed by concrete crushing in the compression zone. The cracks were closely spaced along the span and their number was similar to that in beam C. It worth mentioning that the first cracks were initiated within the splice region indicating effective bond behaviour due to the 90-degree hooked end. Also, providing 90-degree hooked splice in beam C20/90 increased the cracking load to 20-kN, which is twice the cracking load in the rest of test beams in group C. This significant increase was attributed to more effective contribution of the increased reinforcement area along the splice extension and consequent increase of stiffness.

Adding the polypropylene fibers was effective in improving the cracking patterns and increasing the number of cracks at failure. However, beam P20 was an exception as the cracking behaviour was similar to that in beam C20. The improvements due to the use of fibers can be expressed in terms of increased cracking loads compared to the counterpart beams in group C, increased number of more closely spaced cracks at failure and altering the mode of failure to more favourable ductile modes. For instant, beam P40 did not suffer from stress concentration at the end of the splice as in beam C40. Instead, a splitting crack along the splice developed at about 90 percent of the ultimate load. The load continued to increase due to the contribution of the fibers and the beam finally failed due to concrete crushing. Beam P20 failed in a similar fashion as the load continued to increase after the development of a splitting crack. The crack became wider as the applied load increased until the beam failed without crushing of concrete. Providing hooked ends in beams P20/45 and P20/90 enabled a superior cracking behaviour with regard to the number of cracks and the ductile failure due to steel yielding followed by concrete crushing.

All beams in group S failed in a ductile manner. Tension steel in all beams, except beam S20, had yielded before failure. Beam S20 failed due to the development of a splitting crack along the splice. Flexure cracks continued to propagate upwards until the beams failed due to concrete crushing. Beam S20/90 failed due to steel yielding followed by the appearance of a splitting crack immediately prior to failure that occurred due to concrete crushing in the compression zone.

4.3 Stiffness and ductility

Fig. 6 shows the load-midspan deflection response of test beams. In all groups, the post-cracking

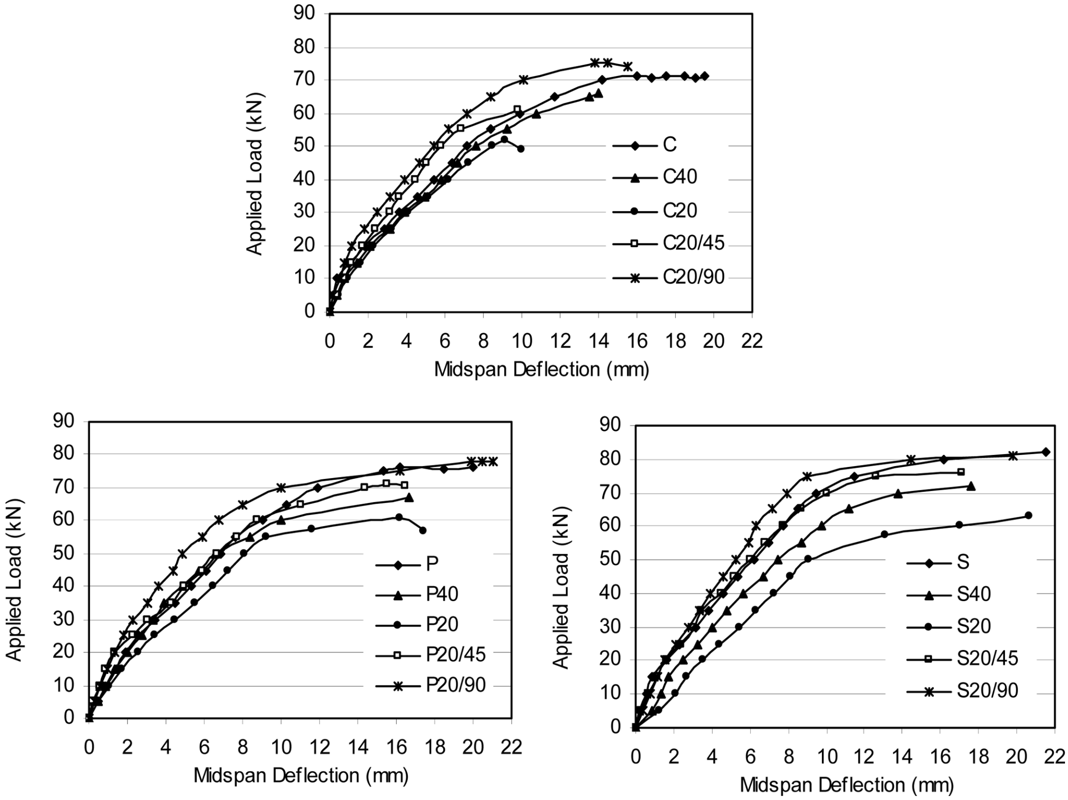

Fig. 6 Load-midspan defection curves

stiffness of the spliced beams without hooks was reduced due to the splice. This was attributed to the tendency to crack at the free ends of the spliced bars. The initial cracks were relatively wider than the initial cracks in the counterpart control beam due to stress concentration at the splice ends. Providing end hooks seemed to improve the post-cracking stiffness especially the 90-degree hook. The ductility of test beams was expressed in terms of the ductility index defined as the ratio of midspan deflection at ultimate load (d_u) and that at the yield load (d_y). The ductility index values reported in Table 4 indicate that the ductility improved due to the application of fibers and further increased due to the use of hooks especially the 90-degree-hook. The yielding of steel was characterized by a plateau in the load-deflection response associated with higher ductility index. The response of beams P40, P20 and S20 was also ductile due to the implementation of fibers that assisted in carrying the load after the development of a splitting bond crack along the splice.

4.4 Ultimate loads

Table 4 reports the experimental ultimate loads of test beams and their relative values expressed as the ultimate load of a test beam divided by the ultimate load of beam C. The relative values show reductions of 7% and 27% in the ultimate loads of beams C40 and C20, respectively. A splice length of $40d_b$ was inadequate to achieve full bond resistance. This result fulfilled the aim stated at the end of section (4.1) concerning the design of test beams. The splice length in beam C40 was an intermediate value between $29.4d_b$ according to Eq. (2) and $49d_b$ according a simplified version of this equation when $(c_b + K_{tr})/d_b = 1.5$. Adopting an intermediate value of $40d_b$ for the splice length had only a minor negative effect on the ultimate load, yet the cracking pattern and mode of failure were not satisfactory. The shorter splice length of $20d_b$ provided with a 90-degree end hook in beam C20/90 demonstrated a superior behaviour compared to the control beam in terms of the ultimate load that was 6% higher, the increased post-cracking stiffness and the increased number of cracks at failure besides a favourable ductile mode of failure. Adding the polypropylene and steel fibers increased the ultimate loads by 7% and 16% in beams P and S, respectively. While beam P40 ceased to sustain the ultimate load of beam C, beam S40 achieved a slightly higher ultimate load and a ductile mode of failure. On the other hand, the use of steel fibers in beam S20 increased the ultimate load to 89% of that of the control beam. Applying the 45-degree and 90-degree end hooks in beams P20/90 and S20/90 was effective in increasing the ultimate load by 10% and 14%, respectively. This result indicated that splice lengths shorter than those specified by the ACI 318R-08 code might be described in case of steel fiber reinforced concrete.

5. Conclusions

The current work investigated the flexure and bond behaviour of spliced simply supported beam specimens. The influence of the splice length, configuration of the end hook and the type of concrete were the main test parameters. A normal strength concrete mix and two fiber reinforced concrete mixes incorporating steel and polypropylene fibers were used in casting the test specimens. The structural behaviour of test beams in terms of the mode of failure, load-deflection response, cracking loads and ultimate loads was analysed. Based on the obtained test results and analysis, the following main conclusions could be drawn:

1. A splice length that was 36 percent longer than that calculated according to the detailed

equation of the ACI 318R-08 code (Eq. 12.1) yielded a mode of splitting bond failure in plain concrete, while the ultimate load was marginally less than that of the unspliced control beam.
2. A splice that was 30 percent shorter than that calculated according to the detailed equation of the ACI 318R-08 code (Eq. 12.1), yet provided with a 90-degree hook, fulfilled the splice function in plain concrete as the steel yielded before failure and a higher ultimate load was obtained compared to that of the unspliced control beam.
3. Compared to counterpart plain concrete beams, the use of polypropylene fibers increased the ultimate loads by 19 percent and 4 percent when 45-degree and 90-degree end hooks were used, respectively. The corresponding ratios were 27 percent and 8 percent when steel fibers were used.
4. The use of either polypropylene or steel fibers ensured a more favourable ductile failure in all test beams even those that did not demonstrate yielding of tension steel. Those beams were able to maintain load increase after the development of a splitting crack along the splice due to the contribution of the fibers in carrying the tensile force.
5. Combining steel or polypropylene fiber reinforced concrete and 90-degree end hooks can provide a superior flexure performance of spliced beams compared to similar unspliced plain concrete beams.

References

ACI 408.3-01/408.3R-01 (2001), "Splice and development length of high relative rib area reinforcing bars in tension", *ACI Committee 408*, 6.

ACI 544.1R-96 (2002), "Report on fiber reinforced concrete", *ACI Committee 544*, 66.

ACI 408R-03 (2003), "Bond and development of straight reinforcing bars in tension", *ACI Committee 408*, 49.

ACI 408.2R-92 (2005), "Bond under cyclic loads", *ACI Committee 408*, 32.

ACI 407R-07 (2007), "Report on fiber-reinforced polymer (FRP) reinforcement for concrete structures", *ACI Committee 440*, 104.

ACI 318R-08 (2008), "Building code requirements for structural concrete (318-08) and commentary", *ACI Committee 318*, 471.

ASTM A820 "Standard Specification for Steel Fibers for Fiber-Reinforced Concrete", 4.

Azizinamini, A., Stark, M., Roller, J. and Ghosh, S. (1993), "Bond performance of reinforcing bars embedded in high-strength concrete", *ACI Struct. J.*, **90**(5), 554-561.

BS-EN 197-1 (2000), "Cement: composition, specifications, and conformity criteria for common cements", *British Standards*, 52.

Bilal, S.H., Harajli, M.H. and Ghaida, J. (2001), "Effect of fiber reinforcement on bond strength of tension lap splices in high strength concrete", *ACI Struct. J.*, **98**(5), 638-647.

Bilal, S.H., Soudki, K.A., Harajli, M.H. and Rteil, A. (2004), "Experimental and analytical evaluation of bond strength of reinforcement in fiber reinforced polymer-wrapped high strength concrete beams", *ACI Struct. J.*, **101**(6), 747-754.

Bilal, S.H., Abou Haidar, E.Y. and Harahjli, M.H. (2011), "Effect of steel fibers on bond strength of hooked bars in normal strength concrete", *ACI Struct. J.*, **108**(1), 42-50.

Darwin, D. and Graham, E.K. (1993), "Effect of deformation height and spacing on bond strength of reinforcing bars", *ACI Struct. J.*, **90**(6), 646-657.

Esfahani, R. and Rangan, V. (1998), "Bond between normal strength and high-strength concrete (HSC) and reinforcing bars in splices in beams", *ACI Struct. J.*, **95**(3), 272-280.

Ezeldin, A.S. and Balaguru, P.N. (1989), "Bond behavior of normal and high strength fiber concrete", *ACI Mater. J.*, **86**(5), 515-524.

FIB (2000), "Bond of reinforcement in concrete", State-of-the-art Report, *FIB Bulletin 10*, Switzerland.

Harajli, M.H., Hout, M. and Jalkh, W. (1995), "Local bond stress-slip behavior of reinforcing bars embedded in

plain and fiber concrete", *ACI Mater. J.*, **92**(4), 343-354.
Harajli, M.H. and Salloukh, K.A. (1997), "Effect of fibers on development/splice strength of reinforcing bars in tension", *ACI Mater. J.*, **94**(4), 317-324.
Harajli, M.H., Bilal, S.H. and Rteil, A.A. (2004), "Effect of confinement on bond strength between steel bars and concrete", *ACI Struct. J.*, **101**(5), 595-603.
Harahjli, M.H. (2005), "Bond strengthening of steel bars using external FRP confinement: Implications on the static and cyclic response of RC members", *ACI Special Publication*, **230**, 579-596.
Harajli, M.H. (2006), "Effect of confinement using steel, FRC, or FRP on the bond stress-slip response of steel bars under cyclic loading", *Mater. Struct.*, **39**, 621-634.
Leung, H.Y. (2003), "Flexural performance of concrete beam splices with different surrounding concretes", *Struct. Survey*, **21**(5), 216-224.
Mehmet, K., Turk, K. and Zulfu, C.U. (2010) "Investigation of bond between lap-spliced steel bar and self-compacting concrete: the role of silica fume", *Can. J. Civ. Eng.*, **37**, 420-428.
Pimanmas, A. and Thai, D.X. (2011), "Response of lap splice of reinforcing bars confined by FRP wrapping: application to nonlinear analysis of RC column", *Struct. Eng. Mech.*, **37**(1), 111-129.
Soroushian, P., Mirza, F. and Alhozaimy, A. (1994), "Bonding of confined steel fiber reinforced concrete to deformed bars", *ACI Mater. J.*, **91**(2), 141-149.
Turk, K. (2003), "Bond strength of reinforcement in splices in beams", *Struct. Eng. Mech.*, **16**(4), 1-9.
Turk, K., Caliskan, S. and Yildirim, M.S. (2005), "Influence of loading condition and reinforcement size on the concrete/reinforcement bond strength", *Struct. Eng. Mech.*, **19**(3), 337-346.
Thai, D.X. and Pimanmas, A. (2011), "Response of lap splice of reinforcing bars confined by FRP wrapping: modelling approach", *Struct. Eng. Mech.*, **37**(1), 95-110.
Zuo, J. and Darwin, D. (2000), "Splice strength of conventional and high relative rib area bars and high strength concrete", *ACI Struct. J.*, **97**(4), 630-641.